



Transverse polarization measurement of Λ hyperons in p Ne collisions at $\sqrt{s_{\text{NN}}} = 68.4$ GeV with the LHCb detector

LHCb collaboration[†]

Abstract

A measurement of the transverse polarization of the Λ and $\bar{\Lambda}$ hyperons in p Ne fixed-target collisions at $\sqrt{s_{\text{NN}}} = 68.4$ GeV is presented using data collected by the LHCb detector. The polarization is studied using the decay $\Lambda \rightarrow p\pi^-$ together with its charge conjugated process, the integrated values measured are

$$P_{\Lambda} = 0.029 \pm 0.019 (\text{stat}) \pm 0.012 (\text{syst}),$$

$$P_{\bar{\Lambda}} = 0.003 \pm 0.023 (\text{stat}) \pm 0.014 (\text{syst}).$$

Furthermore, the results are shown as a function of the Feynman x variable, transverse momentum, pseudorapidity and rapidity of the hyperons, and are compared with previous measurements.

Submitted to JHEP

© 2024 CERN for the benefit of the LHCb collaboration. CC BY 4.0 licence.

[†]Authors are listed at the end of this paper.

1 Introduction

The spontaneous transverse polarization of Λ hyperons was first observed in 1976 in unpolarized fixed-target collisions of protons with an energy of 300 GeV and a beryllium target [1]. This result was in contradiction with the expectation that the large number of final states in high-energy particle production would suppress polarization effects and showed that spin effects contribute significantly even at high-energy. A polarizing fragmentation function, denoted by D_{1T}^\perp , has been proposed in Refs. [2–4] to account for the polarized production of Λ hyperons. The mechanism involving the D_{1T}^\perp function is the same as that used in the framework of the transverse-momentum-dependent unpolarized fragmentation functions (TMDs) to describe the fragmentation of an unpolarized quark into a transversely polarized hadron. The spin and azimuthal asymmetries observed at sufficiently large energy scales cannot be explained by asymmetries at the level of the hard partonic process, instead their origin must lie in soft processes. By maintaining an explicit dependence on the intrinsic partonic motion, TMDs account for spin and momentum correlations at the soft level, potentially explaining the observed asymmetries. Since these functions arise from soft mechanisms, they are difficult to calculate from first principles. Hence, just as with collinear parton distribution functions and fragmentation functions, one possible approach is to determine them from experimental data. Several attempts were made to describe Λ polarization, both on the theoretical and experimental sides, at different accelerators and center-of-mass energies. Particularly relevant are the measurements from the STAR experiment at RHIC [5] and Belle at KEKB [6]. None of these results led to a fully satisfactory answer, and the mechanism giving rise to Λ polarization is still unclear. In this paper, a measurement of transverse Λ and $\bar{\Lambda}$ polarization is presented, using the LHCb experiment in a fixed-target configuration. The polarization is determined using proton-neon ($p\text{Ne}$) data collected in 2017 from collisions at a nucleon-nucleon center-of-mass energy of $\sqrt{s_{\text{NN}}} = 68.4$ GeV, generated by a 2.5 TeV proton beam incident on neon nuclei at rest and corresponding to an integrated luminosity of 24.9 nb^{-1} . The hyperons are reconstructed through the decays $\Lambda \rightarrow p\pi^-$ and $\bar{\Lambda} \rightarrow \bar{p}\pi^+$. The results are obtained as a function of the transverse momentum (p_T) of the hyperon, the pseudorapidity (η), the rapidity (y) and the Feynman variable $x_F = \frac{2 \cdot p_L}{\sqrt{s_{\text{NN}}}}$ (where p_L is the longitudinal momentum of the particle), as a non trivial dependence of the polarization on these variables has been reported in other publications [7].

2 The LHCb detector

The LHCb detector [8, 9] is a single-arm forward spectrometer, designed for the study of particles containing c or b quarks, covering the pseudorapidity range $2 < \eta < 5$. The detector includes: a silicon-strip vertex locator (VELO), three tracking stations of silicon-strip detectors and straw drift tubes, two ring-imaging Cherenkov detectors (RICH) that are able to discriminate between different species of charged hadrons, a calorimeter system consisting of scintillating-pad and preshower detectors, electromagnetic and hadronic calorimeters, and a muon detector composed of alternating layers of iron and multiwire proportional chambers. The System for Measuring the Overlap with Gas (SMOG) [10] enables the injection of gases with a pressure of $\mathcal{O}(10^{-7})$ mbar in the beam pipe section inside the VELO, allowing LHCb to operate as a fixed-target experiment. The SMOG

system thus provides a unique opportunity to study proton-nucleus and nucleus-nucleus collisions with various gaseous targets using the LHC beams. In this configuration, the LHCb acceptance extends to the negative rapidity hemisphere, due to the boost induced by the high-energy proton beam, which points to the positive- z direction.

3 Data sample and analysis strategy

The p Ne sample was taken during the pp data-taking period. Fixed-target events were collected only when a bunch in the beam pointing towards the LHCb detector crossed the interaction region without a corresponding bunch in the beam pointing to the opposite direction. To suppress the remaining pp background, the z -coordinate of the p Ne primary vertex (PV) is required to lie in the fiducial region $z_{\text{PV}} \in [-200, -100] \cup [100, 150]$ mm.¹ Furthermore, events with more than four hits in the VELO stations upstream of the interaction region are rejected. The online event selection is performed by a trigger [11], that requires at least one track reconstructed in the VELO. Since the Λ reconstruction requires two tracks, this trigger condition does not bias the measurement. In the offline selection, the Λ candidates are required to be reconstructed from proton and pion tracks with opposite charge, forming a vertex with a good-quality fit. Protons and pions are required to have a minimum transverse momentum of 100 MeV/ c and a minimum momentum of 2 GeV/ c . Particle identification (PID) requirements based on the information from the RICH detectors are applied to select protons. Finally, to suppress the contribution of nonprompt Λ hyperons, the impact parameter of the Λ candidate with respect to the PV is required to be less than 1.5 mm, which reduces this contribution to about 5%. Figure 1 shows the $p\pi^-$ and $\bar{p}\pi^+$ invariant-mass distributions obtained after all the selection criteria have been applied. The distributions are fitted with the convolution of a Cauchy and a Gaussian function to describe the signal shape and a first-order polynomial to model the background.

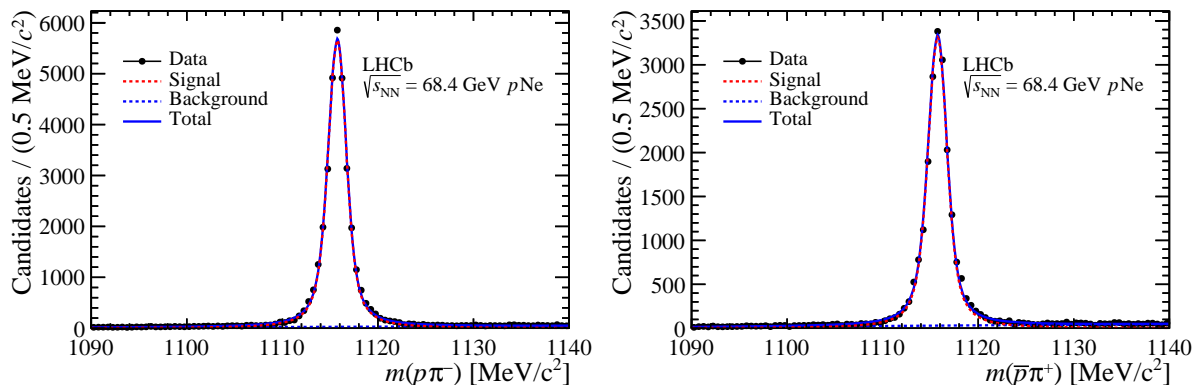


Figure 1: Invariant-mass distributions for (left) Λ and (right) $\bar{\Lambda}$ candidates after all selection requirements are applied. The fit result is overlaid on the data.

¹ $z_{\text{PV}} = 0$ is the z coordinate of the center of the pp interaction region.

The decays $\Lambda \rightarrow p\pi^-$ and $\bar{\Lambda} \rightarrow \bar{p}\pi^+$ exhibit significant parity violation, resulting in large asymmetries in the angular distribution of their decay particles. In particular, the angular distribution of the proton in the Λ rest frame is given by

$$\frac{dN}{d\cos\theta} = \frac{dN_0}{d\cos\theta}(1 + \alpha P_\Lambda \cos\theta), \quad (1)$$

where θ is the angle between the proton momentum and the normal to the production plane spanned by the beam and the Λ momentum directions, $\frac{dN_0}{d\cos\theta}$ is the decay distribution for unpolarized Λ hyperons, P_Λ is the magnitude of the Λ polarization, and α is the value of the parity-violating decay asymmetry for the Λ hyperon. The magnitude of the polarization is determined from a fit to the angular distribution of the proton in 10 bins of $\cos\theta$.

4 Simulation and efficiencies

Efficiencies are estimated using samples of fully simulated events. The simulated decays are reconstructed and analyzed using the same software tools as those used to process the data. In the simulation, Λ hyperons are generated using PYTHIA [12] with a specific LHCb configuration [13] and with colliding-proton beam momentum equal to the momentum per nucleon of the beam and target in the centre-of-mass frame. The decays of unstable particles are described by EVTGEN [14], in which final-state radiation is generated using PHOTOS [15]. The four-momentum of the Λ decay particles is then embedded into p Ne minimum bias events that are generated with the EPOS event generator [16]. The interaction of the generated particles with the detector and its response are implemented using the GEANT4 toolkit [17, 18] as described in Ref. [19].

After reconstruction, the simulated samples are weighted to improve agreement with data. Weights are calculated as the ratio between the normalized data and simulated distributions as a function of p_T , η and z_{PV} with

$$w(p_T, \eta, z_{PV}) = w(p_T, \eta) \cdot w(z_{PV}), \quad (2)$$

where $w(p_T, \eta)$ is evaluated in 6 intervals of transverse momentum between 300 and 2500 MeV/c and 7 intervals of pseudorapidity between 2 and 5. The weights $w(z_{PV})$ are evaluated in 6 intervals between -200 and 150 mm, ignoring the region between -100 and 100 mm outside the fiducial region considered in the analysis. Through the weighting procedure, the simulation is corrected on average by 6% as a function of transverse momentum and pseudorapidity, and by 4% as a function of z_{PV} , for both Λ and $\bar{\Lambda}$ hyperons. Accounting for efficiency factors, Eq. 1 is modified to

$$\frac{dN}{d\cos\theta} = \frac{dN_0}{d\cos\theta}(1 + \alpha P_\Lambda \cos\theta) \times \epsilon(\cos\theta) \times \epsilon_{PID}, \quad (3)$$

where ϵ_{PID} is the particle identification efficiency for the protons, estimated from dedicated calibration data samples and computed as a function of the proton kinematics. The $\epsilon(\cos\theta)$ term is the product of acceptance, reconstruction and selection efficiencies. It is determined using simulation as $\epsilon(\cos\theta) = f_{\text{rec}}(\cos\theta)/f_{\text{gen}}(\cos\theta)$, where f indicates the $\cos\theta$ distribution for generated candidates (f_{gen}), without any detector effect, or for fully reconstructed candidates (f_{rec}), with detector effects included. As the polarization effects

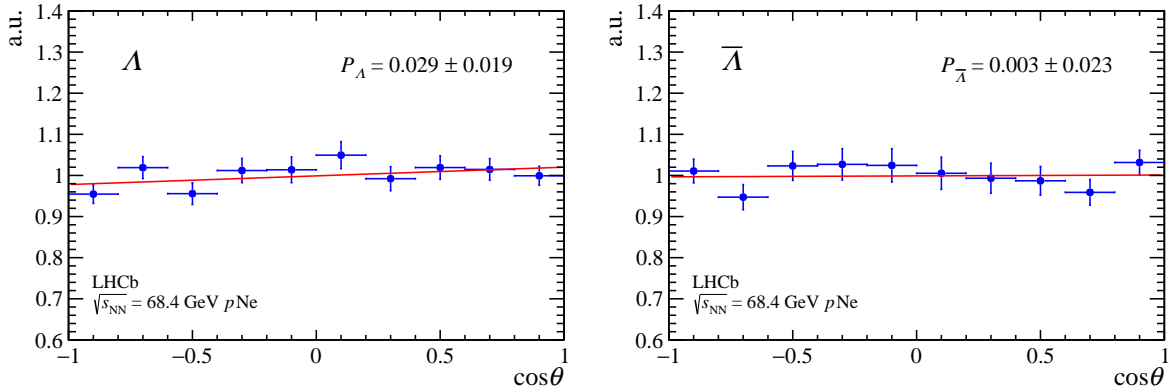


Figure 2: Efficiency-corrected $\cos\theta$ distributions, for (left) Λ and (right) $\bar{\Lambda}$ hyperons. The result of the fit is overlaid (red line).

are not included in the simulation, the generated $\cos\theta$ distribution is uniform. Since only the shape of the distribution is relevant, the efficiency is proportional to the reconstructed $\cos\theta$ distributions, and the generated one is ignored. To correct the angular distributions in data, in each $\cos\theta$ bin, the normalized number of candidates in the data is divided by the normalized number of candidates in the simulated reconstructed sample.

5 Results and systematic uncertainties

The proton angular distributions, after efficiency correction, are shown in Fig. 2. The function $f(\cos\theta) = A(1 + \alpha P_A \cos\theta)$ is fitted to the data distributions, where $\alpha = 0.746 \pm 0.007$ for Λ and $\alpha = -0.757 \pm 0.004$ for $\bar{\Lambda}$ are fixed to their world average value [20]. The magnitude of the polarization is given by the free parameter of the fit shown in Fig. 2.

Several sources of systematic uncertainties are considered. The fit to the invariant-mass distribution is repeated using a double-sided Crystal Ball function [21] instead of the convolution of a Cauchy and a Gaussian function for the signal shape, and a second-order polynomial instead of a first-order one for the background, and the values of the polarization are determined again. The systematic uncertainty is determined as the deviations of these results with respect to those of the default fit. Uncertainties related to the weighting procedure applied to the simulation are taken into consideration by carrying out 100 trials, randomly varying each weight within its uncertainty, calculating new values for the polarization, and taking as systematic uncertainty the largest difference in the polarization values compared to the default one. The choice of the variables used to weight the simulation is also considered; the uncertainty is calculated as the difference between the results obtained by using the track multiplicity and those obtained using the Λ pseudorapidity in the calculation of the weights. The choice of binning for the angular distributions affects the fit results. This is taken into account by repeating the polarization measurements using 5 bins instead of 10 in the angular distribution. Another contribution is associated with the estimation of PID efficiencies. An alternative approach is used, where the particle identification efficiencies are directly estimated from the simulation rather than using dedicated calibration samples. Another systematic uncertainty contribution arises from nonprompt Λ hyperon contamination in the data sample, which is estimated

Table 1: Contributions of systematic uncertainties on the polarization measurement for Λ and $\bar{\Lambda}$ hyperons.

Source	Λ	$\bar{\Lambda}$
Signal estimation	0.007	0.001
Background estimation	0.001	0.010
Kinematic weights	0.001	0.001
Multiplicity dependence	0.001	0.004
Binning of $\cos\theta$ distributions	0.007	0.006
PID efficiencies	0.002	0.005
Nonprompt contamination	0.005	0.002

from simulation to account for 5% of the total yield. To estimate an upper limit on the nonprompt contamination, the impact parameter requirement (which retains approximately 50% of the nonprompt signal) is removed, the measurement is repeated and the difference with the baseline value is taken as systematic uncertainty. The systematic uncertainty due to the external parameter α is found to be negligible. The total systematic uncertainty is computed as the sum in quadrature of each contribution shown in Table 1. The systematic contributions are found to be small and the measurement is dominated by statistical uncertainties. The statistical effect on each systematic contribution is not negligible as reflected in the differences between Λ and $\bar{\Lambda}$ hyperons. The final polarization measurements are

$$P_{\Lambda} = 0.029 \pm 0.019 \text{ (stat)} \pm 0.012 \text{ (syst)},$$

$$P_{\bar{\Lambda}} = 0.003 \pm 0.023 \text{ (stat)} \pm 0.014 \text{ (syst)}.$$

The polarization measurements have also been performed in bins of p_{T} , η , y and x_{F} . The results are shown in Fig. 3 and listed in Table 2. Other experiments with different energies and collision systems have measured the Λ polarization. In its fixed-target configuration, the LHCb experiment covers an energy and kinematic range that is largely unexplored. Figure 4 compares and shows the agreement between the results of this paper with measurements from other experiments, including ATLAS [22], an experiment at the M2 beam-line at Fermilab [23], the E799 experiment [24], NA48 [25], and HERA-B [26]. The measurements reported here, and those from HERA-B, cover negative values of x_{F} , so the results are first transformed using the following symmetry of the transverse polarization $P_{\Lambda}(-x_{\text{F}}) = -P_{\Lambda}(x_{\text{F}})$, and then compared with the other measurements.

6 Conclusions

A measurement of transverse polarization of Λ and $\bar{\Lambda}$ hyperons in p Ne collisions at $\sqrt{s_{\text{NN}}} = 68.4$ GeV by the LHCb experiment is presented. This analysis exploits the innovative and unique fixed-target apparatus at LHC. The measurement in a new collision system and region of phase space can provide additional insights on the mechanism of Λ polarization, which can still not be calculated in quantum chromodynamics. The polarization is measured through the decay $\Lambda \rightarrow p\pi^{-}$ and its charge conjugate, and is studied both as integrated values and in different bins of four kinematic variables: p_{T} , η , x_{F} , and y .

The integrated results are

$$P_{\Lambda} = 0.029 \pm 0.019 \text{ (stat)} \pm 0.012 \text{ (syst)} ,$$

$$P_{\bar{\Lambda}} = 0.003 \pm 0.023 \text{ (stat)} \pm 0.014 \text{ (syst)} .$$

The polarization values obtained in this analysis are compatible with previous measurements, in particular with the HERA-B results which cover a similar x_F interval. The agreement is noteworthy considering the different experiments and colliding systems.

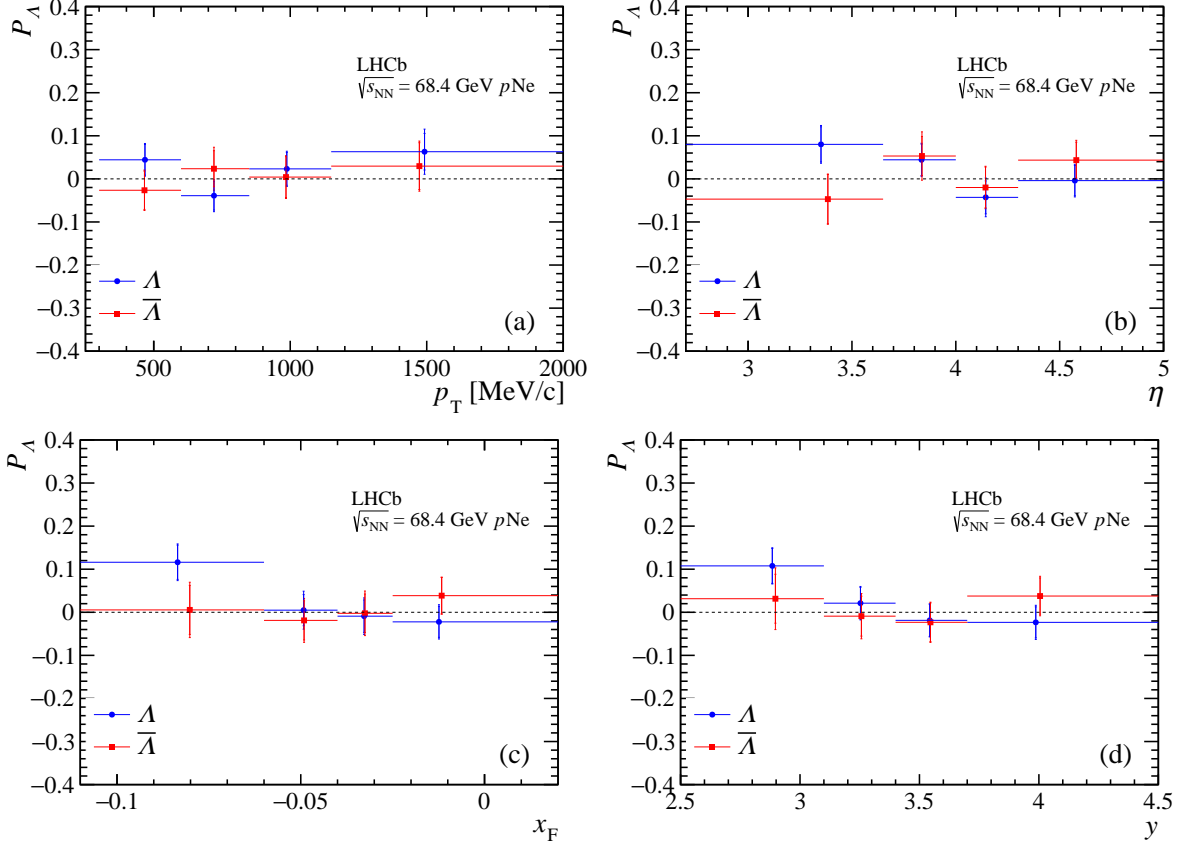


Figure 3: Polarization as a function of (a) p_T , (b) η , (c) x_F and (d) y . Blue (red) symbols are for Λ ($\bar{\Lambda}$). In each plot the data is integrated over the $0.3 < p_T < 3$ GeV/ c and/or $2 < \eta < 5$ kinematic range.

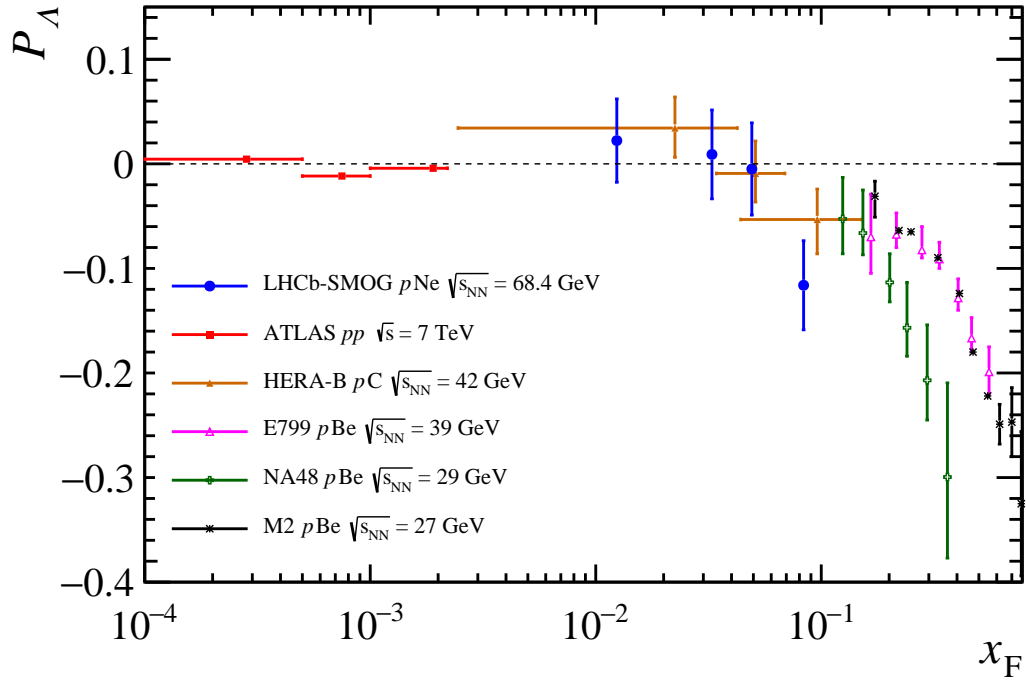


Figure 4: Comparison of polarization as a function of x_F for Λ hyperons obtained in experiments with different energies and with different colliding systems.

Table 2: Polarization in bins of p_T , η , x_F , and y for Λ and $\bar{\Lambda}$. The first uncertainties are statistical and the second are systematic.

	P_Λ	$P_{\bar{\Lambda}}$
p_T [MeV/c]		
[300, 600]	$0.044 \pm 0.035 \pm 0.013$	$-0.026 \pm 0.044 \pm 0.015$
[600, 850]	$-0.039 \pm 0.033 \pm 0.016$	$0.023 \pm 0.042 \pm 0.027$
[850, 1150]	$0.023 \pm 0.038 \pm 0.015$	$0.004 \pm 0.047 \pm 0.015$
[1150, 3000]	$0.063 \pm 0.042 \pm 0.031$	$0.029 \pm 0.054 \pm 0.021$
η		
[2.00, 3.65]	$0.080 \pm 0.040 \pm 0.016$	$-0.047 \pm 0.057 \pm 0.011$
[3.65, 4.00]	$0.044 \pm 0.036 \pm 0.012$	$0.053 \pm 0.045 \pm 0.033$
[4.00, 4.30]	$-0.043 \pm 0.038 \pm 0.024$	$-0.020 \pm 0.047 \pm 0.014$
[4.30, 5.00]	$-0.004 \pm 0.035 \pm 0.014$	$0.043 \pm 0.042 \pm 0.020$
x_F		
[-0.250, -0.060]	$0.116 \pm 0.040 \pm 0.015$	$0.006 \pm 0.057 \pm 0.030$
[-0.060, -0.040]	$0.005 \pm 0.036 \pm 0.025$	$-0.018 \pm 0.045 \pm 0.023$
[-0.040, -0.025]	$-0.009 \pm 0.037 \pm 0.020$	$0.002 \pm 0.045 \pm 0.026$
[-0.025, 0.100]	$-0.022 \pm 0.036 \pm 0.017$	$0.038 \pm 0.042 \pm 0.008$
y		
[2.0, 3.1]	$0.107 \pm 0.040 \pm 0.011$	$0.031 \pm 0.057 \pm 0.044$
[3.1, 3.4]	$0.021 \pm 0.036 \pm 0.013$	$-0.009 \pm 0.046 \pm 0.025$
[3.4, 3.7]	$-0.019 \pm 0.037 \pm 0.010$	$-0.023 \pm 0.045 \pm 0.013$
[3.7, 5.0]	$-0.023 \pm 0.036 \pm 0.016$	$0.038 \pm 0.042 \pm 0.018$

Acknowledgements

We thank Umberto D'Alesio for the fruitful discussions. We express our gratitude to our colleagues in the CERN accelerator departments for the excellent performance of the LHC. We thank the technical and administrative staff at the LHCb institutes. We acknowledge support from CERN and from the national agencies: CAPES, CNPq, FAPERJ and FINEP (Brazil); MOST and NSFC (China); CNRS/IN2P3 (France); BMBF, DFG and MPG (Germany); INFN (Italy); NWO (Netherlands); MNiSW and NCN (Poland); MCID/IFA (Romania); MICINN (Spain); SNSF and SER (Switzerland); NASU (Ukraine); STFC (United Kingdom); DOE NP and NSF (USA). We acknowledge the computing resources that are provided by CERN, IN2P3 (France), KIT and DESY (Germany), INFN (Italy), SURF (Netherlands), PIC (Spain), GridPP (United Kingdom), CSCS (Switzerland), IFIN-HH (Romania), CBPF (Brazil), and Polish WLCG (Poland). We are indebted to the communities behind the multiple open-source software packages on which we depend. Individual groups or members have received support from ARC and ARDC (Australia); Key Research Program of Frontier Sciences of CAS, CAS PIFI, CAS CCEPP, Fundamental Research Funds for the Central Universities, and Sci. & Tech. Program of Guangzhou (China); Minciencias (Colombia); EPLANET, Marie Skłodowska-Curie Actions, ERC and NextGenerationEU (European Union); A*MIDEX, ANR, IPhU and Labex P2IO, and Région Auvergne-Rhône-Alpes (France); AvH Foundation (Germany); ICSC (Italy); GVA, XuntaGal, GENCAT, Inditex, InTalent and Prog. Atracción Talento, CM (Spain); SRC (Sweden); the Leverhulme Trust, the Royal Society and UKRI (United Kingdom).

References




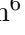








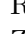

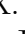



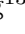

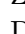



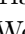



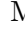
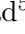
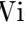

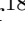
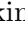




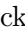
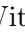




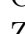

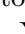
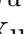




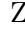

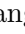
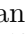
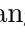
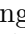
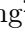

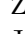
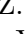
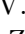
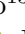
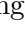
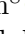
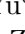

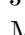
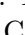
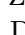

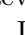





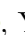

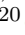

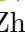

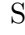
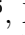
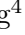
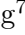




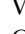
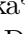

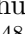


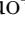



- [1] G. Bunce *et al.*, Λ^0 hyperon polarization in inclusive production by 300-GeV protons on beryllium, *Phys. Rev. Lett.* **36** (1976) 1113.
- [2] D. Boer, C. J. Bomhof, D. S. Hwang, and P. J. Mulders, *Spin asymmetries in jet-hyperon production at LHC*, *Phys. Lett.* **B659** (2008) 127.
- [3] D. Boer, *Transverse Lambda polarization at LHC*, [arXiv:0907.1610](https://arxiv.org/abs/0907.1610).
- [4] P. J. Mulders and R. D. Tangerman, *The complete tree-level result up to order $1/Q$ for polarized deep-inelastic lepton production*, *Nuclear Physics* **B461** (1996) 197–237.
- [5] T. Gao, *Measurement of transverse polarization of $\Lambda/\bar{\Lambda}$ within jet in pp collisions at STAR*, [arXiv:2402.01168](https://arxiv.org/abs/2402.01168).
- [6] Y. Guan *et al.*, *Observation of transverse $\Lambda/\bar{\Lambda}$ hyperon polarization in e^+e^- annihilation at Belle*, *Physical Review Letters* **122** (2019) 042001, [arXiv:1808.05000](https://arxiv.org/abs/1808.05000).
- [7] A. Airapetian, N. Akopov, and Z. Akopov, *Transverse polarization of Λ hyperons from quasireal photoproduction on nuclei*, *Phys. Rev.* **D90** (2014) 072007.
- [8] LHCb collaboration, A. A. Alves Jr. *et al.*, *The LHCb detector at the LHC*, *JINST* **3** (2008) S08005.
- [9] LHCb collaboration, R. Aaij *et al.*, *LHCb detector performance*, *Int. J. Mod. Phys.* **A30** (2015) 1530022, [arXiv:1412.6352](https://arxiv.org/abs/1412.6352).
- [10] LHCb collaboration, R. Aaij *et al.*, *Precision luminosity measurements at LHCb*, *JINST* **9** (2014) P12005, [arXiv:1410.0149](https://arxiv.org/abs/1410.0149).
- [11] R. Aaij *et al.*, *The LHCb trigger and its performance in 2011*, *JINST* **8** (2013) P04022, [arXiv:1211.3055](https://arxiv.org/abs/1211.3055).
- [12] T. Sjöstrand, S. Mrenna, and P. Skands, *A brief introduction to PYTHIA 8.1*, *Comput. Phys. Commun.* **178** (2008) 852, [arXiv:0710.3820](https://arxiv.org/abs/0710.3820).
- [13] I. Belyaev *et al.*, *Handling of the generation of primary events in Gauss, the LHCb simulation framework*, *J. Phys. Conf. Ser.* **331** (2011) 032047.
- [14] D. J. Lange, *The EvtGen particle decay simulation package*, *Nucl. Instrum. Meth.* **A462** (2001) 152.
- [15] P. Golonka and Z. Was, *PHOTOS Monte Carlo: a precision tool for QED corrections in Z and W decays*, *The European Physical Journal* **C45** (2006) 97.
- [16] T. Pierog *et al.*, *EPOS LHC: Test of collective hadronization with data measured at the CERN Large Hadron Collider*, *Phys. Rev.* **C92** (2015) 034906.
- [17] Geant4 collaboration, S. Agostinelli *et al.*, *Geant4: A simulation toolkit*, *Nucl. Instrum. Meth.* **A506** (2003) 250.

- [18] Geant4 collaboration, J. Allison *et al.*, *Geant4 developments and applications*, IEEE Trans. Nucl. Sci. **53** (2006) 270.
- [19] M. Clemencic *et al.*, *The LHCb simulation application, Gauss: Design, evolution and experience*, J. Phys. Conf. Ser. **331** (2011) 032023.
- [20] Particle Data Group, R. L. Workman *et al.*, *Review of particle physics*, Prog. Theor. Exp. Phys. **2022** (2022) 083C01.
- [21] T. Skwarnicki, *A study of the radiative cascade transitions between the Upsilon-prime and Upsilon resonances*, PhD thesis, Institute of Nuclear Physics, Krakow, 1986, DESY-F31-86-02.
- [22] ATLAS collaboration, G. Aad *et al.*, *Measurement of the transverse polarization of Λ and $\bar{\Lambda}$ hyperons produced in proton-proton collisions at $\sqrt{s} = 7$ TeV using the ATLAS detector*, Phys. Rev. **D91** (2015) 032004, [arXiv:1412.1692](https://arxiv.org/abs/1412.1692).
- [23] B. Lundberg *et al.*, *Polarization in inclusive Λ and $\bar{\Lambda}$ production at large p_T* , Phys. Rev. **D40** (1989) 3557.
- [24] E. J. Ramberg *et al.*, *Polarization of Λ and $\bar{\Lambda}$ produced by 800-GeV protons*, Phys. Lett. **B338** (1994) 403.
- [25] NA48 collaboration, A. Tkachev, *A measurement of the transverse polarization of Λ hyperons produced in inelastic pN -reactions at 450 GeV proton energy*, Nucl. Phys. B Proc. Suppl. **75** (1999) 45.
- [26] HERA-B collaboration, I. Abt *et al.*, *Polarization of Λ and $\bar{\Lambda}$ in 920-GeV fixed-target proton-nucleus collisions*, Phys. Lett. **B638** (2006) 415, [arXiv:hep-ex/0603047](https://arxiv.org/abs/hep-ex/0603047).

LHCb collaboration

R. Aaij³⁶ , A.S.W. Abdelmotteleb⁵⁵ , C. Abellan Beteta⁴⁹ , F. Abudinén⁵⁵ ,
T. Ackernley⁵⁹ , A. A. Adefisoye⁶⁷ , B. Adeva⁴⁵ , M. Adinolfi⁵³ , P. Adlarson⁷⁹ ,
C. Agapopoulou¹³ , C.A. Aidala⁸⁰ , Z. Ajaltouni¹¹ , S. Akar⁶⁴ , K. Akiba³⁶ ,
P. Albicocco²⁶ , J. Albrecht¹⁸ , F. Alessio⁴⁷ , M. Alexander⁵⁸ , Z. Aliouche⁶¹ ,
P. Alvarez Cartelle⁵⁴ , R. Amalric¹⁵ , S. Amato³ , J.L. Amey⁵³ , Y. Amhis^{13,47} ,
L. An⁶ , L. Anderlini²⁵ , M. Andersson⁴⁹ , A. Andreianov⁴² , P. Andreola⁴⁹ ,
M. Andreotti²⁴ , D. Andreou⁶⁷ , A. Anelli^{29,p} , D. Ao⁷ , F. Archilli^{35,v} ,
M. Argenton²⁴ , S. Arguedas Cuendis⁹ , A. Artamonov⁴² , M. Artuso⁶⁷ ,
E. Aslanides¹² , R. Ataide Da Silva⁴⁸ , M. Atzeni⁶³ , B. Audurier¹⁴ , D. Bacher⁶² ,
I. Bachiller Perea¹⁰ , S. Bachmann²⁰ , M. Bachmayer⁴⁸ , J.J. Back⁵⁵ ,
P. Baladron Rodriguez⁴⁵ , V. Balagura¹⁴ , W. Baldini²⁴ , H. Bao⁷ ,
J. Baptista de Souza Leite⁵⁹ , M. Barbetti^{25,m} , I. R. Barbosa⁶⁸ , R.J. Barlow⁶¹ ,
M. Barnyakov²³ , S. Barsuk¹³ , W. Barter⁵⁷ , M. Bartolini⁵⁴ , J. Bartz⁶⁷ ,
J.M. Basels¹⁶ , G. Bassi³³ , B. Batsukh⁵ , A. Bay⁴⁸ , A. Beck⁵⁵ , M. Becker¹⁸ ,
F. Bedeschi³³ , I.B. Bediaga² , S. Belin⁴⁵ , V. Bellee⁴⁹ , K. Belous⁴² , I. Belov²⁷ ,
I. Belyaev³⁴ , G. Benane¹² , G. Bencivenni²⁶ , E. Ben-Haim¹⁵ , A. Berezhnoy⁴² ,
R. Bernet⁴⁹ , S. Bernet Andres⁴³ , A. Bertolin³¹ , C. Betancourt⁴⁹ , F. Betti⁵⁷ , J.
Bex⁵⁴ , I.a. Bezshyiko⁴⁹ , J. Bhom³⁹ , M.S. Bieker¹⁸ , N.V. Biesuz²⁴ , P. Billoir¹⁵ ,
A. Biolchini³⁶ , M. Birch⁶⁰ , F.C.R. Bishop¹⁰ , A. Bitadze⁶¹ , A. Bizzeti , T. Blake⁵⁵ ,
F. Blanc⁴⁸ , J.E. Blank¹⁸ , S. Blusk⁶⁷ , V. Bocharnikov⁴² , J.A. Boelhave¹⁸ ,
O. Boente Garcia¹⁴ , T. Boettcher⁶⁴ , A. Bohare⁵⁷ , A. Boldyrev⁴² , C.S. Bolognani⁷⁶ ,
R. Bolzonella^{24,l} , N. Bondar⁴² , F. Borgato^{31,q} , S. Borghi⁶¹ , M. Borsato^{29,p} ,
J.T. Borsuk³⁹ , S.A. Bouchiba⁴⁸ , T.J.V. Bowcock⁵⁹ , A. Boyer⁴⁷ , C. Bozzi²⁴ ,
A. Brea Rodriguez⁴⁸ , N. Breer¹⁸ , J. Brodzicka³⁹ , A. Brossa Gonzalo⁴⁵ , J. Brown⁵⁹ ,
D. Brundu³⁰ , E. Buchanan⁵⁷ , A. Buonauro⁴⁹ , L. Buonincontri^{31,q} , A.T. Burke⁶¹ ,
C. Burr⁴⁷ , A. Butkevich⁴² , J.S. Butter⁵⁴ , J. Buytaert⁴⁷ , W. Byczynski⁴⁷ ,
S. Cadeddu³⁰ , H. Cai⁷² , R. Calabrese^{24,l} , S. Calderon Ramirez⁹ , L. Calefice⁴⁴ ,
S. Cali²⁶ , M. Calvi^{29,p} , M. Calvo Gomez⁴³ , P. Camargo Magalhaes^{2,z} , J.
I. Cambon Bouzas⁴⁵ , P. Campana²⁶ , D.H. Campora Perez⁷⁶ ,
A.F. Campoverde Quezada⁷ , S. Capelli²⁹ , L. Capriotti²⁴ , R. Caravaca-Mora⁹ ,
A. Carbone^{23,j} , L. Carcedo Salgado⁴⁵ , R. Cardinale^{27,n} , A. Cardini³⁰ ,
P. Carniti^{29,p} , L. Carus²⁰ , A. Casais Vidal⁶³ , R. Caspary²⁰ , G. Casse⁵⁹ ,
J. Castro Godinez⁹ , M. Cattaneo⁴⁷ , G. Cavallero^{24,47} , V. Cavallini^{24,l} , S. Celani²⁰ ,
D. Cervenkov⁶² , S. Cesare^{28,o} , A.J. Chadwick⁵⁹ , I. Chahrouh⁸⁰ , M. Charles¹⁵ ,
Ph. Charpentier⁴⁷ , E. Chatzianagnostou³⁶ , C.A. Chavez Barajas⁵⁹ , M. Chefdeville¹⁰ ,
C. Chen¹² , S. Chen⁵ , Z. Chen⁷ , A. Chernov³⁹ , S. Chernyshenko⁵¹ ,
V. Chobanova⁷⁸ , S. Cholak⁴⁸ , M. Chruszcz³⁹ , A. Chubykin⁴² , V. Chulikov⁴² ,
P. Ciambone²⁶ , X. Cid Vidal⁴⁵ , G. Ciezarek⁴⁷ , P. Cifra⁴⁷ , P.E.L. Clarke⁵⁷ ,
M. Clemencic⁴⁷ , H.V. Cliff⁵⁴ , J. Closier⁴⁷ , C. Cocha Toapaxi²⁰ , V. Coco⁴⁷ ,
J. Cogan¹² , E. Cogneras¹¹ , L. Cojocariu⁴¹ , P. Collins⁴⁷ , T. Colombo⁴⁷ ,
A. Comerma-Montells⁴⁴ , L. Congedo²² , A. Contu³⁰ , N. Cooke⁵⁸ , I. Corredoira⁴⁵ ,
A. Correia¹⁵ , G. Corti⁴⁷ , J.J. Cottee Meldrum⁵³ , B. Couturier⁴⁷ , D.C. Craik⁴⁹ ,
M. Cruz Torres^{2,g} , E. Curras Rivera⁴⁸ , R. Currie⁵⁷ , C.L. Da Silva⁶⁶ , S. Dadabaev⁴² ,
L. Dai⁶⁹ , X. Dai⁶ , E. Dall'Occo¹⁸ , J. Dalseno⁴⁵ , C. D'Ambrosio⁴⁷ , J. Daniel¹¹ ,
A. Danilina⁴² , P. d'Argent²² , A. Davidson⁵⁵ , J.E. Davies⁶¹ , A. Davis⁶¹ ,
O. De Aguiar Francisco⁶¹ , C. De Angelis^{30,k} , F. De Benedetti⁴⁷ , J. de Boer³⁶ ,
K. De Bruyn⁷⁵ , S. De Capua⁶¹ , M. De Cian^{20,47} , U. De Freitas Carneiro Da Graca^{2,b} ,
E. De Lucia²⁶ , J.M. De Miranda² , L. De Paula³ , M. De Serio^{22,h} , P. De Simone²⁶ 

M. Korolev⁴² ID, I. Kostiuk³⁶ ID, O. Kot⁵¹ ID, S. Kotriakhova ID, A. Kozachuk⁴² ID,
P. Kravchenko⁴² ID, L. Kravchuk⁴² ID, M. Kreps⁵⁵ ID, P. Krovovny⁴² ID, W. Krupa⁶⁷ ID,
W. Krzemien⁴⁰ ID, O.K. Kshyvanskyi⁵¹ ID, J. Kubat²⁰ ID, S. Kubis⁷⁷ ID, M. Kucharczyk³⁹ ID,
V. Kudryavtsev⁴² ID, E. Kulikova⁴² ID, A. Kupsc⁷⁹ ID, B. K. Kutsenko¹² ID, D. Lacarrere⁴⁷ ID,
A. Lai³⁰ ID, A. Lampis³⁰ ID, D. Lancierini⁵⁴ ID, C. Landesa Gomez⁴⁵ ID, J.J. Lane¹ ID,
R. Lane⁵³ ID, C. Langenbruch²⁰ ID, J. Langer¹⁸ ID, O. Lantwin⁴² ID, T. Latham⁵⁵ ID,
F. Lazzari^{33,t} ID, C. Lazzeroni⁵² ID, R. Le Gac¹² ID, R. Lefèvre¹¹ ID, A. Leflat⁴² ID,
S. Legotin⁴² ID, M. Lehuraux⁵⁵ ID, E. Lemos Cid⁴⁷ ID, O. Leroy¹² ID, T. Lesiak³⁹ ID,
B. Leverington²⁰ ID, A. Li⁴ ID, H. Li⁷⁰ ID, K. Li⁸ ID, L. Li⁶¹ ID, P. Li⁴⁷ ID, P.-R. Li⁷¹ ID, Q.
Li^{5,7} ID, S. Li⁸ ID, T. Li^{5,d} ID, T. Li⁷⁰ ID, Y. Li⁸ ID, Y. Li⁵ ID, Z. Lian⁴ ID, X. Liang⁶⁷ ID,
S. Libralon⁴⁶ ID, C. Lin⁷ ID, T. Lin⁵⁶ ID, R. Lindner⁴⁷ ID, V. Lisovskyi⁴⁸ ID, R. Litvinov^{30,47} ID,
F. L. Liu¹ ID, G. Liu⁷⁰ ID, K. Liu⁷¹ ID, S. Liu^{5,7} ID, Y. Liu⁵⁷ ID, Y. Liu⁷¹ ID, Y. L. Liu⁶⁰ ID,
A. Lobo Salvia⁴⁴ ID, A. Loi³⁰ ID, J. Lomba Castro⁴⁵ ID, T. Long⁵⁴ ID, J.H. Lopes³ ID,
A. Lopez Huertas⁴⁴ ID, S. López Soliño⁴⁵ ID, C. Lucarelli^{25,m} ID, D. Lucchesi^{31,q} ID,
M. Lucio Martinez⁷⁶ ID, V. Lukashenko^{36,51} ID, Y. Luo⁶ ID, A. Lupato³¹ ID, E. Luppi^{24,l} ID,
K. Lynch²¹ ID, X.-R. Lyu⁷ ID, G. M. Ma⁴ ID, R. Ma⁷ ID, S. Maccolini¹⁸ ID, F. Machefert¹³ ID,
F. Maciuc⁴¹ ID, B. Mack⁶⁷ ID, I. Mackay⁶² ID, L. M. Mackey⁶⁷ ID, L.R. Madhan Mohan⁵⁴ ID, M.
M. Madurai⁵² ID, A. Maevskiy⁴² ID, D. Magdalinski³⁶ ID, D. Maisuzenko⁴² ID,
M.W. Majewski³⁸ ID, J.J. Malczewski³⁹ ID, S. Malde⁶² ID, L. Malentacca⁴⁷ ID, A. Malinin⁴² ID,
T. Maltsev⁴² ID, G. Manca^{30,k} ID, G. Mancinelli¹² ID, C. Mancuso^{28,13,o} ID,
R. Manera Escalero⁴⁴ ID, D. Manuzzi²³ ID, D. Marangotto^{28,o} ID, J.F. Marchand¹⁰ ID,
R. Marcheviski⁴⁸ ID, U. Marconi²³ ID, S. Mariani⁴⁷ ID, C. Marin Benito⁴⁴ ID, J. Marks²⁰ ID,
A.M. Marshall⁵³ ID, G. Martelli^{32,r} ID, G. Martellotti³⁴ ID, L. Martinazzoli⁴⁷ ID,
M. Martinelli^{29,p} ID, D. Martinez Santos⁴⁵ ID, F. Martinez Vidal⁴⁶ ID, A. Massafferri² ID,
R. Matev⁴⁷ ID, A. Mathad⁴⁷ ID, V. Matiunin⁴² ID, C. Matteuzzi⁶⁷ ID, K.R. Mattioli¹⁴ ID,
A. Mauri⁶⁰ ID, E. Maurice¹⁴ ID, J. Mauricio⁴⁴ ID, P. Mayencourt⁴⁸ ID, M. Mazurek⁴⁰ ID,
M. McCann⁶⁰ ID, L. McConnell²¹ ID, T.H. McGrath⁶¹ ID, N.T. McHugh⁵⁸ ID, A. McNab⁶¹ ID,
R. McNulty²¹ ID, B. Meadows⁶⁴ ID, G. Meier¹⁸ ID, D. Melnychuk⁴⁰ ID, F. M. Meng⁴ ID,
M. Merk^{36,76} ID, A. Merli⁴⁸ ID, L. Meyer Garcia⁶⁵ ID, D. Miao^{5,7} ID, H. Miao⁷ ID,
M. Mikhasenko^{17,f} ID, D.A. Milanese⁷³ ID, A. Minotti^{29,p} ID, E. Minucci⁶⁷ ID, T. Miralles¹¹ ID,
B. Mitreska¹⁸ ID, D.S. Mitzel¹⁸ ID, A. Modak⁵⁶ ID, A. Mödden¹⁸ ID, R.A. Mohammed⁶² ID,
R.D. Moise¹⁶ ID, S. Mokhnenko⁴² ID, T. Mombächer⁴⁷ ID, M. Monk^{55,1} ID, S. Monteil¹¹ ID,
A. Morcillo Gomez⁴⁵ ID, G. Morello²⁶ ID, M.J. Morello^{33,s} ID, M.P. Morgenthaler²⁰ ID,
A.B. Morris⁴⁷ ID, A.G. Morris¹² ID, R. Mountain⁶⁷ ID, H. Mu⁴ ID, Z. M. Mu⁶ ID,
E. Muhammad⁵⁵ ID, F. Muheim⁵⁷ ID, M. Mulder⁷⁵ ID, K. Müller⁴⁹ ID, F. Muñoz-Rojas⁹ ID,
R. Murta⁶⁰ ID, P. Naik⁵⁹ ID, T. Nakada⁴⁸ ID, R. Nandakumar⁵⁶ ID, T. Nanut⁴⁷ ID, I. Nasteva³ ID,
M. Needham⁵⁷ ID, N. Neri^{28,o} ID, S. Neubert¹⁷ ID, N. Neufeld⁴⁷ ID, P. Neustroev⁴² ID,
J. Nicolini^{18,13} ID, D. Nicotra⁷⁶ ID, E.M. Niel⁴⁸ ID, N. Nikitin⁴² ID, P. Nogarolli³ ID, P. Nogga¹⁷ ID,
N.S. Nolte⁶³ ID, C. Normand⁵³ ID, J. Novoa Fernandez⁴⁵ ID, G. Nowak⁶⁴ ID, C. Nunez⁸⁰ ID, H. N.
Nur⁵⁸ ID, A. Oblakowska-Mucha³⁸ ID, V. Obraztsov⁴² ID, T. Oeser¹⁶ ID, S. Okamura^{24,l} ID,
A. Okhotnikov⁴² ID, O. Okhrimenko⁵¹ ID, R. Oldeman^{30,k} ID, F. Oliva⁵⁷ ID, M. Olocco¹⁸ ID,
C.J.G. Onderwater⁷⁶ ID, R.H. O'Neil⁵⁷ ID, J.M. Oalora Goicochea³ ID, P. Owen⁴⁹ ID,
A. Oyanguren⁴⁶ ID, O. Ozcelik⁵⁷ ID, K.O. Padeken¹⁷ ID, B. Pagare⁵⁵ ID, P.R. Pais²⁰ ID,
T. Pajero⁴⁷ ID, A. Palano²² ID, M. Palutan²⁶ ID, G. Panshin⁴² ID, L. Paolucci⁵⁵ ID,
A. Papanestis⁵⁶ ID, M. Pappagallo^{22,h} ID, L.L. Pappalardo^{24,l} ID, C. Pappenheimer⁶⁴ ID,
C. Parkes⁶¹ ID, B. Passalacqua²⁴ ID, G. Passaleva²⁵ ID, D. Passaro^{33,s} ID, A. Pastore²² ID,
M. Patel⁶⁰ ID, J. Patoc⁶² ID, C. Patrignani^{23,j} ID, A. Paul⁶⁷ ID, C.J. Pawley⁷⁶ ID,
A. Pellegrino³⁶ ID, J. Peng^{5,7} ID, M. Pepe Altarelli²⁶ ID, S. Perazzini²³ ID, D. Pereima⁴² ID, H.
Pereira Da Costa⁶⁶ ID, A. Pereiro Castro⁴⁵ ID, P. Perret¹¹ ID, A. Perro⁴⁷ ID, K. Petridis⁵³ ID,
A. Petrolini^{27,n} ID, J. P. Pfaller⁶⁴ ID, H. Pham⁶⁷ ID, L. Pica³³ ID, M. Piccini³² ID,

J. Wagner¹⁸ , J. Walsh³³ , E.J. Walton^{1,55} , G. Wan⁶ , C. Wang²⁰ , G. Wang⁸ , J. Wang⁶ , J. Wang⁵ , J. Wang⁴ , J. Wang⁷² , M. Wang²⁸ , N. W. Wang⁷ , R. Wang⁵³ , X. Wang⁸ , X. Wang⁷⁰ , X. W. Wang⁶⁰ , Y. Wang⁶ , Z. Wang¹³ , Z. Wang⁴ , Z. Wang²⁸ , J.A. Ward^{55,1} , M. Waterlaet⁴⁷ , N.K. Watson⁵² , D. Websdale⁶⁰ , Y. Wei⁶ , J. Wendel⁷⁸ , B.D.C. Westhenry⁵³ , D.J. White⁶¹ , M. Whitehead⁵⁸ , A.R. Wiederhold⁵⁵ , D. Wiedner¹⁸ , G. Wilkinson⁶² , M.K. Wilkinson⁶⁴ , M. Williams⁶³ , M.R.J. Williams⁵⁷ , R. Williams⁵⁴ , F.F. Wilson⁵⁶ , W. Wislicki⁴⁰ , M. Witek³⁹ , L. Witola²⁰ , C.P. Wong⁶⁶ , G. Wormser¹³ , S.A. Wotton⁵⁴ , H. Wu⁶⁷ , J. Wu⁸ , Y. Wu⁶ , K. Wyllie⁴⁷ , S. Xian⁷⁰ , Z. Xiang⁵ , Y. Xie⁸ , A. Xu³³ , J. Xu⁷ , L. Xu⁴ , L. Xu⁴ , M. Xu⁵⁵ , Z. Xu¹¹ , Z. Xu⁷ , Z. Xu⁵ , D. Yang⁴ , K. Yang⁶⁰ , S. Yang⁷ , X. Yang⁶ , Y. Yang^{27,n} , Z. Yang⁶ , Z. Yang⁶⁵ , V. Yeroshenko¹³ , H. Yeung⁶¹ , H. Yin⁸ , C. Y. Yu⁶ , J. Yu⁶⁹ , X. Yuan⁵ , E. Zaffaroni⁴⁸ , M. Zavertyaev¹⁹ , M. Zdybal³⁹ , C. Zeng^{5,7} , M. Zeng⁴ , C. Zhang⁶ , D. Zhang⁸ , J. Zhang⁷ , L. Zhang⁴ , S. Zhang⁶⁹ , S. Zhang⁶ , Y. Zhang⁶ , Y. Z. Zhang⁴ , Y. Zhao²⁰ , A. Zharkova⁴² , A. Zhelezov²⁰ , S. Z. Zheng⁶ , X. Z. Zheng⁴ , Y. Zheng⁷ , T. Zhou⁶ , X. Zhou⁸ , Y. Zhou⁷ , V. Zhovkovska⁵⁵ , L. Z. Zhu⁷ , X. Zhu⁴ , X. Zhu⁸ , V. Zhukov¹⁶ , J. Zhuo⁴⁶ , Q. Zou^{5,7} , D. Zuliani^{31,q} , G. Zunica⁴⁸ .

¹*School of Physics and Astronomy, Monash University, Melbourne, Australia*

²*Centro Brasileiro de Pesquisas Físicas (CBPF), Rio de Janeiro, Brazil*

³*Universidade Federal do Rio de Janeiro (UFRJ), Rio de Janeiro, Brazil*

⁴*Center for High Energy Physics, Tsinghua University, Beijing, China*

⁵*Institute Of High Energy Physics (IHEP), Beijing, China*

⁶*School of Physics State Key Laboratory of Nuclear Physics and Technology, Peking University, Beijing, China*

⁷*University of Chinese Academy of Sciences, Beijing, China*

⁸*Institute of Particle Physics, Central China Normal University, Wuhan, Hubei, China*

⁹*Consejo Nacional de Rectores (CONARE), San Jose, Costa Rica*

¹⁰*Université Savoie Mont Blanc, CNRS, IN2P3-LAPP, Annecy, France*

¹¹*Université Clermont Auvergne, CNRS/IN2P3, LPC, Clermont-Ferrand, France*

¹²*Aix Marseille Univ, CNRS/IN2P3, CPPM, Marseille, France*

¹³*Université Paris-Saclay, CNRS/IN2P3, IJCLab, Orsay, France*

¹⁴*Laboratoire Leprince-Ringuet, CNRS/IN2P3, Ecole Polytechnique, Institut Polytechnique de Paris, Palaiseau, France*

¹⁵*LPNHE, Sorbonne Université, Paris Diderot Sorbonne Paris Cité, CNRS/IN2P3, Paris, France*

¹⁶*I. Physikalisches Institut, RWTH Aachen University, Aachen, Germany*

¹⁷*Universität Bonn - Helmholtz-Institut für Strahlen und Kernphysik, Bonn, Germany*

¹⁸*Fakultät Physik, Technische Universität Dortmund, Dortmund, Germany*

¹⁹*Max-Planck-Institut für Kernphysik (MPIK), Heidelberg, Germany*

²⁰*Physikalisches Institut, Ruprecht-Karls-Universität Heidelberg, Heidelberg, Germany*

²¹*School of Physics, University College Dublin, Dublin, Ireland*

²²*INFN Sezione di Bari, Bari, Italy*

²³*INFN Sezione di Bologna, Bologna, Italy*

²⁴*INFN Sezione di Ferrara, Ferrara, Italy*

²⁵*INFN Sezione di Firenze, Firenze, Italy*

²⁶*INFN Laboratori Nazionali di Frascati, Frascati, Italy*

²⁷*INFN Sezione di Genova, Genova, Italy*

²⁸*INFN Sezione di Milano, Milano, Italy*

²⁹*INFN Sezione di Milano-Bicocca, Milano, Italy*

³⁰*INFN Sezione di Cagliari, Monserrato, Italy*

³¹*INFN Sezione di Padova, Padova, Italy*

³²*INFN Sezione di Perugia, Perugia, Italy*

³³*INFN Sezione di Pisa, Pisa, Italy*

- ³⁴ INFN Sezione di Roma La Sapienza, Roma, Italy
- ³⁵ INFN Sezione di Roma Tor Vergata, Roma, Italy
- ³⁶ Nikhef National Institute for Subatomic Physics, Amsterdam, Netherlands
- ³⁷ Nikhef National Institute for Subatomic Physics and VU University Amsterdam, Amsterdam, Netherlands
- ³⁸ AGH - University of Krakow, Faculty of Physics and Applied Computer Science, Kraków, Poland
- ³⁹ Henryk Niewodniczanski Institute of Nuclear Physics Polish Academy of Sciences, Kraków, Poland
- ⁴⁰ National Center for Nuclear Research (NCBJ), Warsaw, Poland
- ⁴¹ Horia Hulubei National Institute of Physics and Nuclear Engineering, Bucharest-Magurele, Romania
- ⁴² Affiliated with an institute covered by a cooperation agreement with CERN
- ⁴³ DS4DS, La Salle, Universitat Ramon Llull, Barcelona, Spain
- ⁴⁴ ICCUB, Universitat de Barcelona, Barcelona, Spain
- ⁴⁵ Instituto Galego de Física de Altas Enerxías (IGFAE), Universidade de Santiago de Compostela, Santiago de Compostela, Spain
- ⁴⁶ Instituto de Física Corpuscular, Centro Mixto Universidad de Valencia - CSIC, Valencia, Spain
- ⁴⁷ European Organization for Nuclear Research (CERN), Geneva, Switzerland
- ⁴⁸ Institute of Physics, Ecole Polytechnique Fédérale de Lausanne (EPFL), Lausanne, Switzerland
- ⁴⁹ Physik-Institut, Universität Zürich, Zürich, Switzerland
- ⁵⁰ NSC Kharkiv Institute of Physics and Technology (NSC KIPT), Kharkiv, Ukraine
- ⁵¹ Institute for Nuclear Research of the National Academy of Sciences (KINR), Kyiv, Ukraine
- ⁵² University of Birmingham, Birmingham, United Kingdom
- ⁵³ H.H. Wills Physics Laboratory, University of Bristol, Bristol, United Kingdom
- ⁵⁴ Cavendish Laboratory, University of Cambridge, Cambridge, United Kingdom
- ⁵⁵ Department of Physics, University of Warwick, Coventry, United Kingdom
- ⁵⁶ STFC Rutherford Appleton Laboratory, Didcot, United Kingdom
- ⁵⁷ School of Physics and Astronomy, University of Edinburgh, Edinburgh, United Kingdom
- ⁵⁸ School of Physics and Astronomy, University of Glasgow, Glasgow, United Kingdom
- ⁵⁹ Oliver Lodge Laboratory, University of Liverpool, Liverpool, United Kingdom
- ⁶⁰ Imperial College London, London, United Kingdom
- ⁶¹ Department of Physics and Astronomy, University of Manchester, Manchester, United Kingdom
- ⁶² Department of Physics, University of Oxford, Oxford, United Kingdom
- ⁶³ Massachusetts Institute of Technology, Cambridge, MA, United States
- ⁶⁴ University of Cincinnati, Cincinnati, OH, United States
- ⁶⁵ University of Maryland, College Park, MD, United States
- ⁶⁶ Los Alamos National Laboratory (LANL), Los Alamos, NM, United States
- ⁶⁷ Syracuse University, Syracuse, NY, United States
- ⁶⁸ Pontifícia Universidade Católica do Rio de Janeiro (PUC-Rio), Rio de Janeiro, Brazil, associated to ³
- ⁶⁹ School of Physics and Electronics, Hunan University, Changsha City, China, associated to ⁸
- ⁷⁰ Guangdong Provincial Key Laboratory of Nuclear Science, Guangdong-Hong Kong Joint Laboratory of Quantum Matter, Institute of Quantum Matter, South China Normal University, Guangzhou, China, associated to ⁴
- ⁷¹ Lanzhou University, Lanzhou, China, associated to ⁵
- ⁷² School of Physics and Technology, Wuhan University, Wuhan, China, associated to ⁴
- ⁷³ Departamento de Física, Universidad Nacional de Colombia, Bogota, Colombia, associated to ¹⁵
- ⁷⁴ Eotvos Lorand University, Budapest, Hungary, associated to ⁴⁷
- ⁷⁵ Van Swinderen Institute, University of Groningen, Groningen, Netherlands, associated to ³⁶
- ⁷⁶ Universiteit Maastricht, Maastricht, Netherlands, associated to ³⁶
- ⁷⁷ Tadeusz Kosciuszko Cracow University of Technology, Cracow, Poland, associated to ³⁹
- ⁷⁸ Universidade da Coruña, A Coruña, Spain, associated to ⁴³
- ⁷⁹ Department of Physics and Astronomy, Uppsala University, Uppsala, Sweden, associated to ⁵⁸
- ⁸⁰ University of Michigan, Ann Arbor, MI, United States, associated to ⁶⁷
- ⁸¹ Departement de Physique Nucleaire (SPhN), Gif-Sur-Yvette, France

^a Universidade de Brasília, Brasília, Brazil

^b Centro Federal de Educação Tecnológica Celso Suckow da Fonseca, Rio De Janeiro, Brazil

^c Hangzhou Institute for Advanced Study, UCAS, Hangzhou, China

^d School of Physics and Electronics, Henan University, Kaifeng, China

- ^e *LIP6, Sorbonne Universite, Paris, France*
^f *Excellence Cluster ORIGINS, Munich, Germany*
^g *Universidad Nacional Autónoma de Honduras, Tegucigalpa, Honduras*
^h *Università di Bari, Bari, Italy*
ⁱ *Università degli studi di Bergamo, Bergamo, Italy*
^j *Università di Bologna, Bologna, Italy*
^k *Università di Cagliari, Cagliari, Italy*
^l *Università di Ferrara, Ferrara, Italy*
^m *Università di Firenze, Firenze, Italy*
ⁿ *Università di Genova, Genova, Italy*
^o *Università degli Studi di Milano, Milano, Italy*
^p *Università degli Studi di Milano-Bicocca, Milano, Italy*
^q *Università di Padova, Padova, Italy*
^r *Università di Perugia, Perugia, Italy*
^s *Scuola Normale Superiore, Pisa, Italy*
^t *Università di Pisa, Pisa, Italy*
^u *Università della Basilicata, Potenza, Italy*
^v *Università di Roma Tor Vergata, Roma, Italy*
^w *Università di Siena, Siena, Italy*
^x *Università di Urbino, Urbino, Italy*
^y *Universidad de Alcalá, Alcalá de Henares, Spain*
^z *Facultad de Ciencias Físicas, Madrid, Spain*
^{aa} *Department of Physics/Division of Particle Physics, Lund, Sweden*
[†] *Deceased*